Novel Core-Shell Non-Sintered Lightweight Aggregate Concrete for Better Properties in Wallboard

Chaoming PANG (pangchao@seu.edu.cn)
Southeast University
Xinxin MENG
Commercial Aircraft Corporation of China (China)
Chunpeng ZHANG
Southeast University
Jinlong PAN
Southeast University

Research Article

Keywords: core-shell non-sintered lightweight aggregate, porous lightweight aggregate concrete, thermal insulation, drying shrinkage, pore structure.

Posted Date: July 8th, 2021

DOI: https://doi.org/10.21203/rs.3.rs-638127/v1

Abstract

Shrinkage of foam concrete can easily cause cracking and thus makes it difficult for a manufacturer to maintain quality. The density of lightweight aggregate concrete is too high to meet specifications for lightweight and thermal insulation for wallboard. Two types of concrete with dry density in the range 1000–1200 kg/m^3 for use in wallboard were designed and prepared using foam and lightweight aggregate. The properties of porous lightweight aggregate concrete with core-shell non-sintered lightweight aggregate were compared with sintered lightweight aggregate concrete along with several dimensions. The two aggregates were similar in particle size, density, and strength. The effects of each aggregate on the workability, compressive strength, dry shrinkage, and thermal conductivity of the lightweight concrete were analyzed and compared. Pore structures were determined by mercury intrusion porosimetry and X-ray computed tomography. Compressive strength ranged from 7.8 to 11.8 MPa, and thermal conductivity coefficients ranged from 0.193 to 0.219 W/m/K for both types of concrete. The results showed that the core-shell non-sintered lightweight aggregate bonded better with the paste matrix at the interface transition zone and had a better pore structure than the sintered lightweight aggregate concrete. Slump flow of the core-shell non-sintered lightweight aggregate concrete was about 20% greater than that of the sintered lightweight aggregate concrete, 28d compressive strength was about 10% greater, drying shrinkage was about 10% less, and thermal conductivity was less. Porous lightweight aggregate concrete using core-shell non-sintered lightweight aggregate performs well when used in wallboard because of its low density, high thermal insulation, and improved strength.

1. Introduction

Lightweight materials that have high thermal insulation were increasingly applied to the modern construction and building industry. Lightweight aggregate concrete (LAC) is concrete that contains lightweight aggregate (LA) and has a density < 1900 kg/m^3, significantly less than the density of ordinary concrete[]. Also, LAC has lower thermal conductivity than ordinary concrete because of its greater porosity[]. Much recent research has focused on reducing the density of LAC and increasing its thermal insulation properties. Techniques include increasing the LA content[] and using ultralight porous LA[]. Ke[] and Gao[] found that a major obstacle to casting concrete with ultralight LA was that the aggregate floated. If the aggregate density is too great or too small, the aggregate will sink or float. To avoid aggregate sinking or floating, the apparent density of LA should match the dry density of the cementitious matrix[].

Foam concrete is another lightweight concrete, in which foam is produced in the cement paste by some suitable foaming agent[,]. Foam concrete has low apparent density and low thermal conductivity; however, it has drawbacks, such as low strength and high drying shrinkage, and it readily absorbs water[,].

Porous lightweight aggregate concrete (PLAC) can be prepared using LA and introducing large numbers of micropores into the concrete. It shrinks less and has less probability of cracking than foam concrete

and is less dense and possesses greater heat insulation than LA concrete. Properties of PLAC include good apparent density, high strength, good thermal insulation[,,,] and good sound absorption[13,]. PLAC aggregate can be sintered ceramsite or other non-sintered LA, crushed waste clay bricks[15], or light aerated concrete waste[14]. Micropores can be introduced using a foaming agent[12,14,15] or an air-entraining agent[13].

Commercial LAs are sintered at about 1200 °C, but sintering consumes a lot of clay and energy. Production of non-sintered LA (NLA), which is cured at room temperature or below 100 °C, reduces clay consumption, saves energy, and reduces emissions. Norlia et al.[] created a lightweight aggregate with a loose bulk density of 813 kg/m³ and compressive strength of 7.83 MPa using ordinary Portland cement and a foaming agent. Peng et al.[] created a non-sintered lightweight aggregate from dredging sediment with a bulk density of 850 kg/m³ and compressive strength of 5 MPa. They added a pore-forming agent to the NLA[16] to improve sound absorption and decrease density, but the bulk density remained at about 850 kg/m^3. Various measures have been taken to reduce the density of NLA, but the bulk density of NLA is generally > 800 kg/m³. Frankovic et al. produced LAC using 100% NLA and found that it had dry density 1490 kg/m^3 and thermal conductivity 0.73 W/m/K, values that are 35% and 46% less than those of normal concrete[]. The higher density and higher thermal conductivity of NLA, compared to SLA, limit its use in lightweight concrete, so there is correspondingly little research interest in NLA. It is necessary to decrease the bulk density of NLA and improve its thermal insulation properties to make its use viable.

A core-shell non-sintered lightweight aggregate (CNLA) with relatively low bulk density 500–750 kg/m^3 has recently been developed. Our thorough literature review showed only one study of low-density CNLA, by Feras[]. Feras produced CNLA with bulk densities 510–650 kg/m^3 and compressive strengths 1.0–2.5 MPa. The CNLA consisted of cores of expanded perlite particles surrounded by outer shells consisting of perlite powders with fly ash and cement[]. When cement and silica fume were subsequently used to recoat the surface layer, the compressive strength of the CNLA with bulk density 608 kg/m^3 increased to 3.55 MPa[].

We used a novel CNLA consisting of an expanded polystyrene (EPS) sphere with a diameter of 3–4 mm as the core, surrounded by an outer shell consisting of fly ash and cement, as shown in Fig. 1. The EPS spheres greatly improve the thermal insulation properties of LA. Its bulk density, compressive strength, and other aggregate properties can be set to specified levels by varying core size and adjusting shell performance. The bulk compressive strength of the aggregate was in the range 2.5–7.0 MPa when the density was in the range 580–720 kg/m^3[]. The loose bulk density of NLA can be reduced to approximately 500 kg/m³ if the inner core diameter of the EPS spheres is increased. The properties of CNLA, at the same density or strength, greatly exceed those of the NLA produced by Feras, who used expanded perlite particles as the inner core[22].

Two sets of samples of porous lightweight aggregate concrete (PLAC) were prepared using core-shell CNLA or SLA. The characteristics and properties of the two sets of samples were analyzed and

compared.

2. Materials And Experimental Program

2.1. Raw Materials

PLAC specimens were prepared using Chinese standard P.II 42.5R Portland cement with a specific surface area of 362 m^2/kg. Class 1 fly ash (FA) was used with a 95% water requirement and 1.5% loss on ignition. The chemical composition of the cement and fly ash was determined by X-ray fluorescence, as shown in Table 1. A commercial vegetable protein foaming agent was used to create micropores. The foaming agent was dissolved in water (1:30), and the foam was produced at high pressure; foam properties are shown in Table 2.

Two lightweight coarse aggregates, non-sintered LA and SLA, both with particle size 5–10 mm, were used. The SLA was a commercial clay SLA. We produced the CNLA. Table 3 shows the aggregate properties.

Table 1
Cement composition determined by X-ray fluorescence, wt %.

Oxide	CaO	Al_2O_3	SiO_2	Fe_2O_3	P_2O_5	SO_3	K_2O	Cr	TiO_2	Cl^-	MnO
Cement	51.54	8.16	23.61	3.40	6.44	5.25	1.07	0.15	0.30	0.03	0.05
FA	5.54	24.72	57.77	6.42	1.16	1.14	1.91	0.01	1.22	0.008	0.11

Table 2
Foam properties.

Dilution ratio	Diameter range (μm)	Average diameter (μm)	Stabilization time (min)	Density (kg/m^3)
1:30	70–821	341	140	59

Table 3
LA properties.

Aggregate	Water absorption (%)	Apparent density (kg/m^3)	Loose bulk density (kg/m^3)	Bulk compressive strength (MPa)
SLA	12.5	967	498	1.5
CNLA	18.2	1001	507	1.6

2.2. Specimen Preparation

PLAC is designed for use in thermal insulation wallboard and is therefore required to have low density, high thermal insulation, and adequate strength for the application. In practice, low-cost manufacture and combinations of readily available materials are essential qualities. In this study, the desired dry density was 1000 kg/m³(density level 1000) or 1200 kg/m³(density level 1200), and the corresponding desired compressive strengths were 7.5 MPa and 10 MPa. Polycarboxylic acid water reducer was used to ensure PLAC fluidity; A small amount of natural sand with a density of 2600 kg/m³ was used as the fine aggregate to reduce the manufacturing cost. The mixture proportions of PLAC were calculated to obtain these values (Table 4 and Table 5). In mixtures with the same density, the volume contents of LA were the same, but the mass contents of LA were slightly different due to the difference in densities.

Table 4
Mix proportions of concrete constituents.

Density Level	Water/Binder	FA (%)	LA (%)	Sand (volume ratio of aggregate) (%)	Foam (volume ratio) (%)	Water reducer (quality ratio of binder) (%)
1000	0.33	20	30	20	35	0.8
1200	0.30	20	35	20	30	1.0

Table 5
Mix proportions of concrete samples.

No.[1]	Target density (kg/m^3)	Cement (kg/m^3)	FA (kg/m^3)	Water (kg/m^3)	LA (kg/m^3)	Sand (kg/m^3)	Foam (kg/m^3)	Water reducer (kg/m^3)
S1000	1000	304	76	125	290	195	21	3.04
N1000	1000	304	76	125	300	195	21	3.04
S1200	1200	344	86	129	338	228	18	4.30
N1200	1200	344	86	129	350	228	18	4.30

[1]S = SLA, N = CNLA; 1000 and 1200 are the densities.

PLAC was prepared using prefabricated foam as follows. (1) The lightweight aggregate was presoaked for 1 h (SLA) or 15 min (CNLA); the aggregates absorb water at different rates. (2) Cement, water (reduced by the quantity of water used for foaming), water reducer, and presoaked LA were steadily mixed for 2 min. (3) The prefabricated foam was added to the mixer, and the fresh PLAC was mixed for 2 min. During this stage, the difference between the actual wet apparent density and the theoretical wet apparent density was controlled to be < 50 kg/m^3. (4) The fresh PLAC was put into the molds. The specimens were demolded after curing for 24 h in the atmosphere and placed in a standard curing room at 20 ± 2 ºC with relative humidity > 95% for different periods, depending on the subsequent testing.

2.3 Performance Characterization

A conventional concrete slump test was used to characterize workability according to Chinese National Standard GB/T 50080 – 2016; the slump cone was only once filled up without tamping because all concrete specimens were highly flowable.

Three cubes with sides of 100 mm were used for compressive strength testing for each sample. A 3–5 kN/s loading force was used according to Chinese National Standard GB/T 50081 – 2019.

Drying shrinkage of PLAC was measured according to Chinese National Standard GB/T 50082 – 2009 with prisms of size 100 mm×100 mm×400 mm. After curing for 2 d in a standard curing room, the specimens were moved into a dry curing room at temperature 20 ± 2 ºC and relative humidity 65 ± 5%.

Thermal conductivity of PLAC was measured using the steady-state heat transfer method according to Chinese National Standard GB/T 10294 – 2008, using 2 specimen prisms 300 mm×300 mm×30 mm. The hot side temperature was set to 35 ºC, and the cold side temperature was set to 15 ºC. The equilibrium time before heating was set to 2 h.

The pore structure of the PLAC matrix was determined using mercury intrusion porosimetry (MIP) with measuring pore size > 3.6 nm. An Autopore IV 9500 automated mercury porosimeter was used for MIP; the measurement size range was 3.6 nm–360 μm, and the balance time was set for 20 s. The large pore structure of a specimen prism 50 mm×50 mm×50 mm was calculated using X-ray computed tomography (X-CT). The X-ray voltage and current were 80 kV and 0.20 mA, the detector was 1024×1024 pixels, and the resolution was 62 μm/pixel.

3. Experimental Results And Discussion

3.1. Workability

Table 6
Slump and slump flow diameter of PLAC.

Group	S1000	N1000	S1200	N1200
Slump (mm)	232	267	224	261
Flow diameter (mm)	452	507	411	493

PLAC slump and slump flow diameter are shown in Table 6 and Fig. 2. The slump tests showed that SLA is unstable and tends to float upward. Thus the slump and slump flow diameter performance of PLAC with SLA cannot be improved by an additional water reducer. Figure 2 shows that neither segregation nor delamination occurred in PLAC with CNLA. Table 6 shows that both the slump and slump flow diameter of PLAC with CNLA were greater than those of PLAC with SLA for density levels 1000 or 1200. There are two reasons for this: CNLA is more spherical; and, in both cases, the LA was presoaked and excess moisture was removed before it was used. The SLA became saturated more slowly than the CNLA and

continued to absorb water during mixing, thus reducing the water content of the PLAC matrix. As a result, the slump and slump flow of PLAC with SLA were less than those of PLAC with CNLA.

3.2. Compressive Strength

Figure 3 shows the change in compressive strength during PLAC curing for the different aggregates and two density levels. The data in each aggregate–density category showed very little difference.

Figure 3 shows that the compressive strength for both types of PLAC increased rapidly from 3 d to 7 d; the growth rates were 52% for PLAC with SLA and 42% for PLAC with CNLA. The compressive strength of both types of PLAC increased slowly from 14 d to 28 d: the growth rate was 15.6% for PLAC with CNLA but only 3% for PLAC with SLA.

The samples were dried in an oven at 105 ºC after they had cured for 7 d. Figure 4 shows the change of density with drying time. The density of both types of PLAC markedly decreased after 24 h. The density of PLAC with SLA did not change significantly from 24 h to 72 h, but the density of PLAC with CNLA decreased steadily. This internal curing phenomenon of lightweight aggregates is generally recognized[,]. Absorbed water was slowly released from CNLA because the outer shells of aggregate spheres were thicker and denser than the LA shells and contained many micropores. The released water facilitated continuous internal curing of the concrete and resulted in increased compressive strength of PLAC with CNLA from 14 d to 28 d, which became greater than that of PLAC with SLA. The compressive strength of PLAC with CNLA was slightly greater for each density level.

3.3. Drying Shrinkage

Drying shrinkage is a major concern in lightweight concrete fabrication. We investigated drying shrinkage in both types of LA concrete during curing. Three data points were measured in each sample group, and the data showed little variation. Drying shrinkage during dry curing at 1 d, 3 d, 7 d, 14 d, 21 d, and 28 d is shown in Fig. 5 for both types of PLAC.

Figure 5 shows the change in drying shrinkage for two types of PLAC at two density levels. The drying shrinkage of PLAC is low and ranged from 0.07–0.12% at 28 d. Roslan found that the typical range of drying shrinkage of foamed concrete with 600, 1000, and 1400 kg/m^3 density is between 0.1% and 0.35% of the total volume of the hardened matrix[]. Drying shrinkage of foamed lightweight structural concrete with a density of 1900 kg/m^3 ranged from 0.12–0.15% at 28 d when glycol was used to reduce shrinkage[]. These findings show that PLAC has better drying shrinkage performance than foamed concrete or foamed lightweight structural concrete with similar density.

The drying shrinkage of the 1200 density level LAC is much less than that of the 1000 density level because more foam was used in the 1000 density level concrete. As a result, there are more internal pores in the low-density PLAC and consequently greater water absorption loss. For each density level, the drying shrinkage of the PLAC with CNLA was less than that of PLAC with SLA. Most researchers agree that the

incorporation of presoaked lightweight aggregate as an internal curing agent reduces the drying shrinkage of cementitious composites[,] and that increasing the LA content increases internal curing[]. Water released from LWA increases hydration and alters the pore structure[]. CNLA released more water over a longer period than SLA because it absorbed more water and released moisture more slowly. CNLA is also a cement-based material and therefore compatible with the matrix, which suggests it may bond better with the matrix and thus resist drying shrinkage.

3.4. Thermal Conductivity

Table 7
Thermal conductivity of PLAC with CNLA or SLA.

Group	S1000	N1000	S1200	N1200
Thermal conductivity (W/m/K)	0.205	0.193	0.219	0.207

Table 7 shows the thermal conductivity of the two types of PLAC. Thermal insulation is excellent, and all thermal conductivity coefficients were < 0.22 W/m/K. Tajra obtained thermal conductivity values in the range 0.300–0.317 W/m/K for LAC mixed at approximately the same density as our samples but having higher strength; it was also more expensive[22]. Jones obtained thermal conductivity in the range 0.23–0.42 W/m/K for foam concrete with dry densities of 1000–1200 kg/m^3[]. Ganesan produced foamed concrete samples with densities in the range 700 to 1400 kg/m^3, using additives, and thermal conductivity values in the range 0.24–0.74 W/m/K, with thermal conductivity corresponding to density[]. In general, PLAC produced by mixing LA and foam into the concrete mix had high thermal insulation. The thermal conductivity of PLAC with a density of 1200 kg/m^3 was greater than that of PLAC with a density of 1000 kg/m^3 because there were fewer pores. The cement paste was thus more compact in the denser PLAC, and the heat was transferred quickly. Thermal conductivity of PLAC with CNLA was less than for PLAC with SLA because the EPS foam balls used in CNLA acted as thermal insulation, resulting in lower thermal conductivity for the composite PLAC with CNLA.

3.5. Pore Structure

The pore size distribution and pore diameters of the samples are shown in Table 8. $D_{Average}$ and D_{Median} are average pore diameter and median pore diameter, and $D_{Probable}$ is the most probable pore diameter.

Table 8
Porosity of PLAC determined by mercury intrusion.

No.	Pore size distribution (%)				Pore statistic (nm)			Porosity (%)	
	<50 nm	50–200 nm	200–1000 nm	>1000 nm	$D_{Average}$	D_{Median}	$D_{Probable}$	By MIP	By X-CT
S1000	3.9	11.0	8.5	11.8	119.3	336.2	120.8	36.3	55.2
N1000	17.1	5.6	3.2	8.1	32.0	77.5	90.3	34.0	29.8
S1200	3.3	11.8	8.1	11.5	90.2	265.8	77.1	34.7	52.1
N1200	18.0	6.2	3.0	3.8	28.7	77.1	50.4	32.1	28.1

Figure 6 shows the cumulative porosity of the PLAC samples (CNLA and SLA), and Fig. 7 shows the relationship between pore size and the log differential of the mercury intrusion in the concrete. Figure 8 shows the internal microstructure of the samples obtained by X-CT. Micropores in the PLAC were mainly distributed in LA. The test results show that there were more micropores in the PLAC with CNLA and that their size distribution range was less than that in the PLAC with SLA and thus the micropores were more homogeneous. Because the CNLA core was EPS, the porosity of PLAC with CNLA included only data from the matrix and the aggregate shells of CNLA. When the porosity of PLAC with SLA was compared with that of PLAC with CNLA in the X-CT images, the former was 24.0–25.4% greater.

Table 8 shows that the porosity of PLAC with density level 1200 was much less than that of PLAC with density level 1000 and that the average pore diameter and the most probable pore size diameter were also less. The table also shows that porosity was very different between the two types of PLAC. The most probable pore size of PLAC with SLA was 77.1 nm and of PLAC with CNLA was 50.4 nm. The average pore size of PLAC with CNLA was also less than that of PLAC with sintered LA.

Pores < 50 nm diameter had little effect, but pores > 50 nm diameter had more damaging effects. Table 8 shows that about 50% of the pores in PLAC with CNLA and about 10% of the pores in PLAC with SLA fell into the nondamaging category. The two-dimensional slices in Fig. 8 show that the aggregates were evenly dispersed. These results are consistent with the test results from mercury intrusion porosimetry. CNLA better absorbs and releases water, and CNLA slowly releases the absorbed water as an internal curing agent and provides water for further cementitious hydration. The release of water makes the aggregate structure more compact and reduces the porosity of the concrete.

Scanning electron microscope (SEM) images are shown in Fig. 9. The images show that the interface transition zone bond between CNLA and the paste matrix was denser than that between SLA and the matrix. This is because the shells of CNLA are also cement paste and therefore similar in substance to the matrix. Feras attributed the increased density of the interface transition zone to internal curing caused by absorbed water stored within the aggregate[31]. The quantity of water stored in CNLA was much

greater than was stored in SLA, which resulted in PLAC with CNLA having better pore structure, better mechanical properties, and lower shrinkage than PLAC with SLA.

4. Summary And Conclusion

In this study, samples of porous lightweight aggregate concrete were prepared using CNLA or SLA. The workability, compressive strength, drying shrinkage, thermal conductivity, and pore structure of two different densities of each type of concrete were extensively investigated. Our results are summarized as follows:

1. An inexpensive PLAC, with excellent performance, was mixed from readily available constituents: cement, a small amount of natural sand, and lightweight aggregate. Its dry density ranged from 1000 to 1200 kg/m^3, and its compressive strength ranged from 7.8 to 11.8 MPa, with shrinkage between 0.07% and 0.12% and thermal conductivity coefficients ranging from 0.193 to 0.219 W/m/K.
2. PLAC with CNLA had better workability, strength and thermal insulation, and lower dry shrinkage, than PLAC with SLA. Its fluidity was about 20% greater, its strength was about 10% greater, and its thermal conductive coefficient and drying shrinkage were about 6% and 11% less.

We drew the following conclusions from our analysis of the experimental results.

1. The CNLA shells bonded strongly to the paste matrix at the transition zone interface when compared to the PLAC with SLA. Mercury intrusion porosimetry and X-CT showed that PLAC with CNLA had fewer pores and a better pore structure than PLAC with SLA, which increased water retention and provided moisture during curing for a longer hydration period.
2. CNLA is an excellent lightweight aggregate. Its properties allow it to meet design specifications by controlling core size and adjusting shell performance, and its loose bulk density can be as low as 500 kg/m³when EPS spheres are used as aggregate. PLAC with CNLA performs better than PLAC with SLA in all respects. It has better workability, superior mechanical properties, less drying shrinkage, lower thermal conductivity, and a better pore structure. Core-shell CNLA saves energy in fabrication because it does not require sintering and therefore does not consume clay.
3. In conclusion, CNLA has the potential for successful practical use in the economical manufacture of lightweight concrete.

Declarations

Acknowledgment

The authors gratefully acknowledge financial support from the National Key Technologies R&D Program of China (2016YFC0701907) and the National Natural Science Foundation of China (grants 51108077).

References

1. Jo B.W., Park S.K., Park J.B.. Properties of concrete made with alkali-activated fly ash lightweight aggregate (AFLA). Cement Concrete & Composites, 2007, 29:128-135.
2. Demirbo R., Gül R.. The effects of expanded perlite aggregate, silica fume and fly ash on the thermal conductivity of lightweight concrete. Cement & Concrete Research, 2003,33(5):723-727.
3. Uysal H, Demirbog˘ a R S, Ahin R and Gül R. The effects of different cement dosages, slumps, and pumice aggregate ratios on the thermal conductivity and density of concrete. Cement & Concrete Research, 2004, 34(5):845-848.
4. Chandra S and Berntsson L Lightweight Aggregate Concrete. Elsevier Science, New York, NY, USA. 2002,21-65.
5. Ke Y., A.-L. Beaucour, et al. Influence of volume fraction and characteristics of lightweight aggregates on the mechanical properties of concrete. Construction & Building Materials, 2009, 23:2821-2829.
6. GaoY L, Zou C. Experimental study on segregation resistance of nanoSiO2 fly ash lightweight aggregate concrete. Construction & Building Materials, 2015, 93:64-69.
7. Cao Z, Zhang L, Yang Z H. Preliminary experimental design of mix proportion of LA foam concrete [C]// Symposium on production and application technology of lightweight aggregate concrete across the Strait. 2012.
8. Tian T, Yan Y, Hu Z, et al. Utilization of original phosphogypsum for the preparation of foam concrete. Construction & Building Materials, 2016, 115:143-152.
9. Narayanan J S, Ramamurthy K. Identification of set-accelerator for enhancing the productivity of foam concrete block manufacture. Construction & Building Materials, 2012, 37(3):144-152.
10. Awang H, Mydin M A O, Roslan A F. Effects of Fibre on Drying Shrinkage, Compressive and Flexural Strength of Lightweight Foamed Concrete. Advanced Materials Research, 2012, 587:144-149.
11. She W, Du Y, Zhao G, Feng P, Zhang Y, Cao X, Influence of coarse fly ash on the performance of foamed concrete and its application in high-speed railway roadbeds. Construction & Building Materials, 2018, 170:153–166.
12. Weigler H, Karl S. Structural lightweight aggregate concrete with reduced density-lightweight aggregate foamed concrete. International Journal of Cement Composites and Lightweight Concrete, 1980, 2(2):101-104.
13. Kim H K, Jeon J H, Lee H K. Workability, and mechanical, acoustic and thermal properties of lightweight aggregate concrete with a high volume of entrained air. Construction & Building Materials, 2012, 29(none):193-200.
14. Qin H, Sun W, Li G, et al. Preparation and Properties of Foam Concrete with Inorganic Lightweight Tailings. Scientific Journal of Materials Science, 2013□3(3):103—107□
15. Ibrahim N M, Salehuddin S, Amat R C, et al. Performance of Lightweight Foamed Concrete with Waste Clay Brick as Coarse Aggregate. APCBEE Procedia, 2013, 5:497-501.
16. Wu H.Q., Zhang T., Pan R.J., et al. Sintering-free preparation of porous ceramsite using low-temperature decomposing pore former and its sound-absorbing performance. Construction and

Building Materials, 2018,171:367–376

17. Ibrahim N M, Qi L, et al. Properties of lightweight bubbles aggregate (LBA) for the replacement of coarse aggregates in concrete. Materials Science Forum, 2014, 803:11-15.
18. Peng X, Zhou Y, Jia R, et al. Preparation of non-sintered lightweight aggregates from dredged sediments and modification of their properties. Construction & Building Materials, 2017, 132:9-20.
19. Frankovicˇ A., Bosiljkov V.B., V. Ducman, Lightweight aggregates made from fly ash using the cold-bond process and their use in lightweight concrete. Materials Technology. 2017,51:267–274
20. Tajra F., Elrahman M.A. Stephan D. Production and properties of cold-bonded aggregate and its applications in concrete: A review. Construction and Building Materials2019,225:29-43.
21. Tajra F., Elrahman M.A., Chung S.Y., et al. Performance assessment of core-shell structured lightweight aggregate produced by cold bonding pelletization process. Construction & Building Materials, 2018, 179:220-231.
22. Tajra F., Elrahman M.A., Lehmann C., et al.Properties of lightweight concrete made with core-shell structured lightweight aggregate . Construction & Building Materials, 2019, 205:39-51.
23. Pang C M, Lu M Y, Sun Y K. Study on Preparation and properties of core-shell structure burning lightweight aggregate. Silicate Bulletin, 2016, 35 (7): 2121-2127.
24. Bentz D P , Snyder K A . Protected paste volume in concrete: Extension to internal curing using saturated lightweight fine aggregate. Cement & Concrete Research, 1999, 29(11):1863-1867.
25. Akhnoukh, Amin K . Internal curing of concrete using lightweight aggregates. Particulate Science and Technology, 2016:1-6.
26. Roslan A F , Awang H , Mydin M A O . Effects of Various Additives on Drying Shrinkage, Compressive and Flexural Strength of Lightweight Foamed Concrete (LFC). Advanced Materials Engineering and Technology, 2013, 626:594-604.
27. Prinya Chindaprasirt, Ubolluk Rattanasak. Shrinkage behavior of structural foam lightweight concrete containing glycol compounds and fly ash. Materials & Design, 2011,32(2):723-727.
28. Esmaeili J , Kasaei J . Effect of Internal Curing Using Lightweight Scoria Fine Aggregates on Autogenous Shrinkage, Strength and Transport Properties of Cement Mortars. Proceedings of the National Academy of Sciences, 2003, 7(3):14269-74.
29. Cusson D , Hoogeveen T. Internal curing of high-performance concrete with pre-soaked fine lightweight aggregate for prevention of autogenous shrinkage cracking . Cement and Concrete Research, 2008, 38(6):757-765.
30. Nahhab A.H., Ketab A.K. Influence of content and maximum size of light expanded clay aggregate on the fresh, strength, and durability properties of self-compacting lightweight concrete reinforced with micro steel fibers , Construction and Building Materials, 2020,233: 117922
31. Ma X.W., Liu J.H., Shi C.J. A review on the use of LWA as an internal curing agent of high performance cement-based materials. Construction and Building Materials, 2019,218:385–393.

32. Jones M.R., McCarthy A., Heat of hydration in foamed concrete: effect of mix constituents and plastic density, Cement and Concrete Research, 2006,36 (6) 1032–1041.
33. Ganesan S., OthumanMydin M.A., MohdYunos M.Y., MohdNawi M.N., Thermal properties of foamed concrete with various densities and additives at ambient temperature, Apply. Mech. Mater. 2015,747: 230–233.

Figures

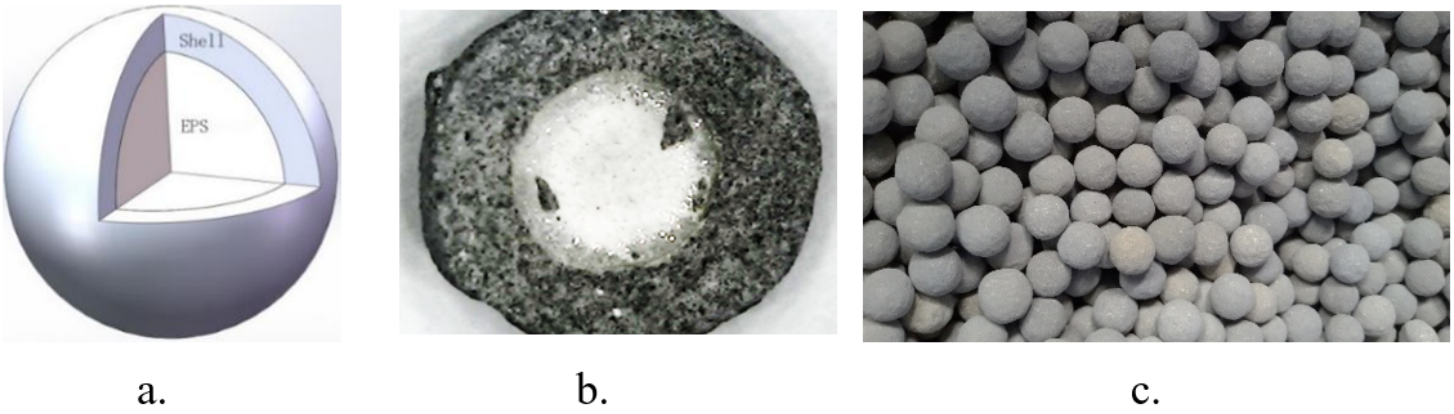

Figure 1

Core-shell non-sintered LA: a. diagram of core-shell; b. photo of EPS core and fly ash–cement shell; c. photo of Core-shell non-sintered LA.

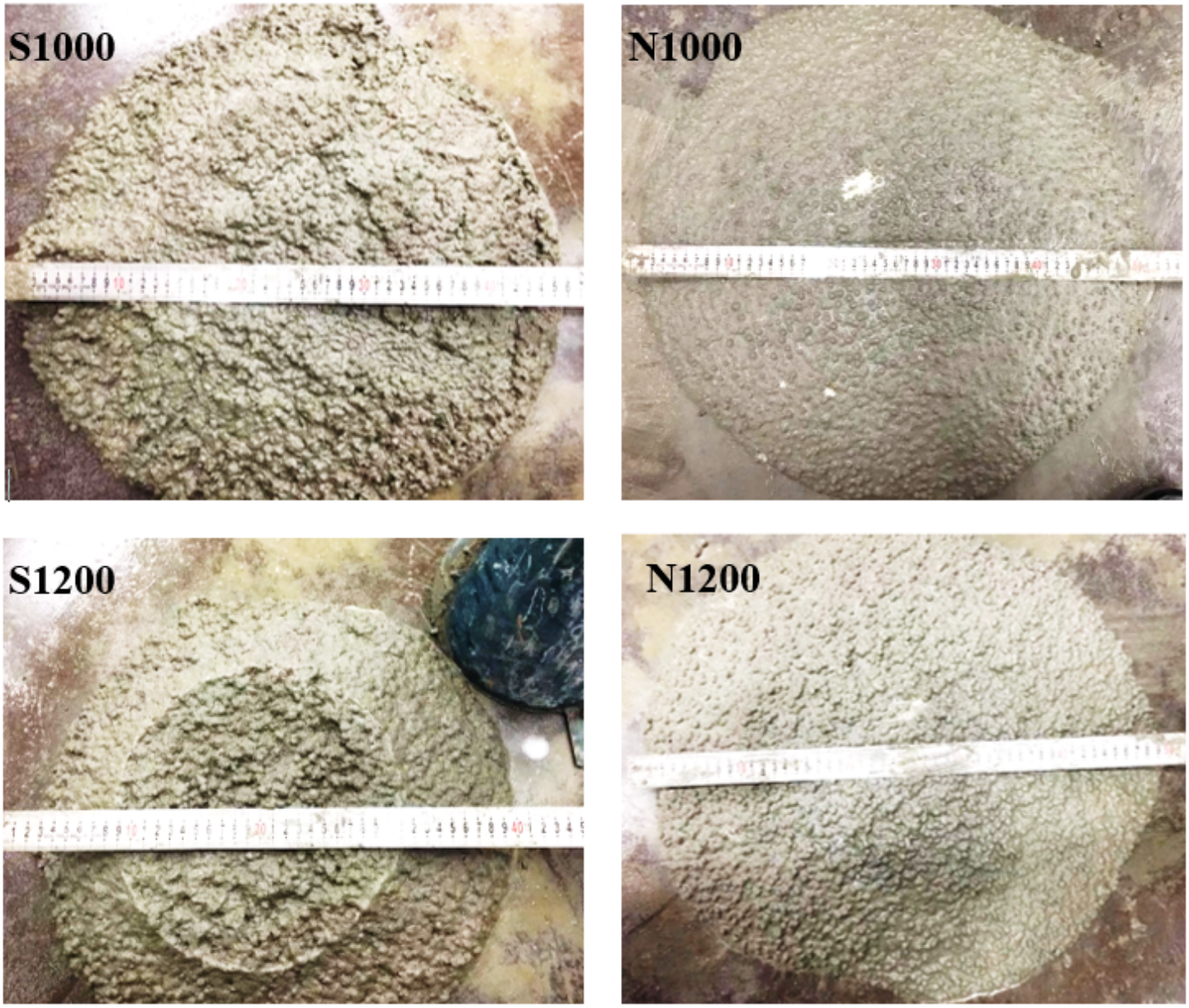

Figure 2

PLAC settling.

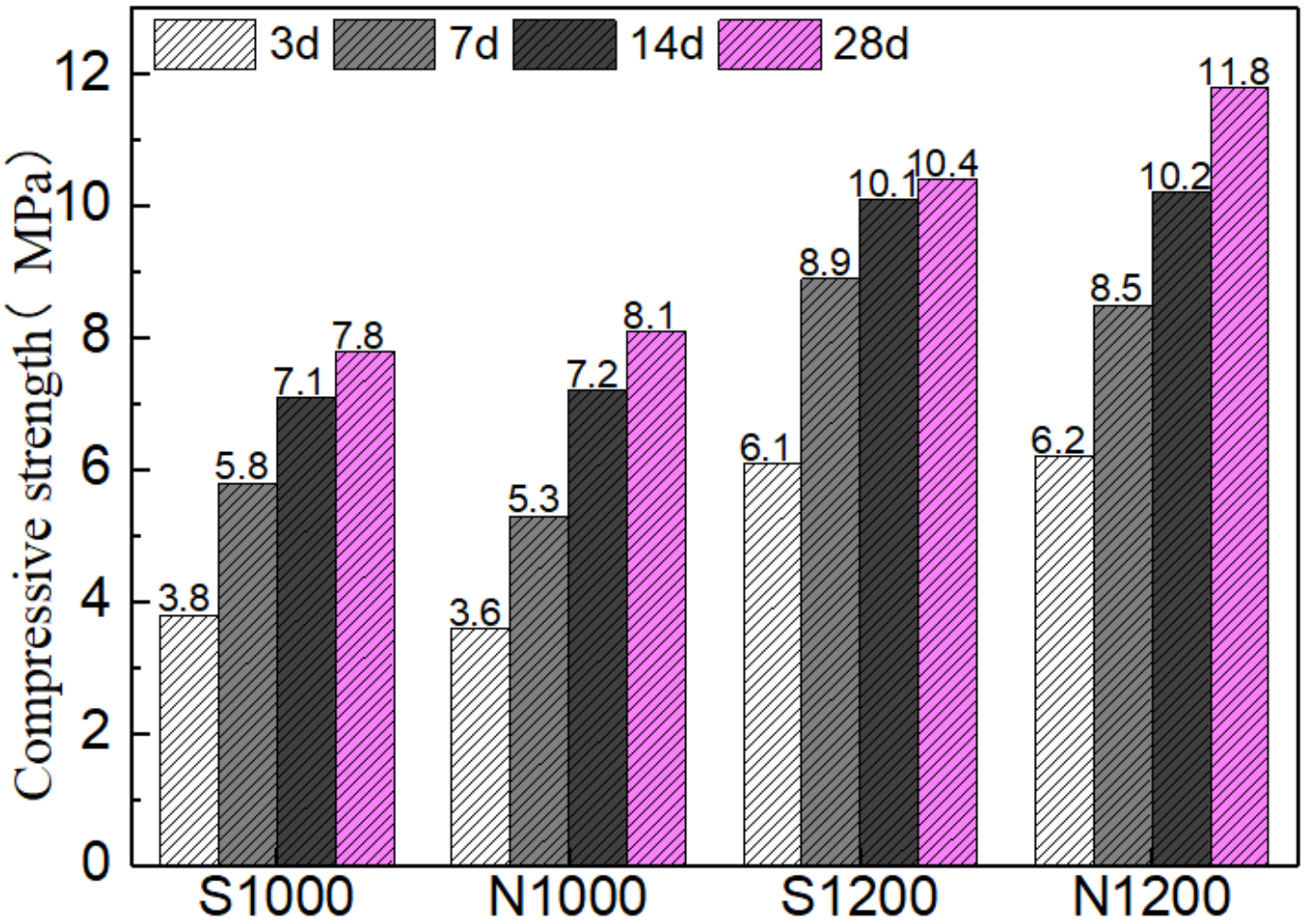

Figure 3

Compressive strength of PLAC specimens.

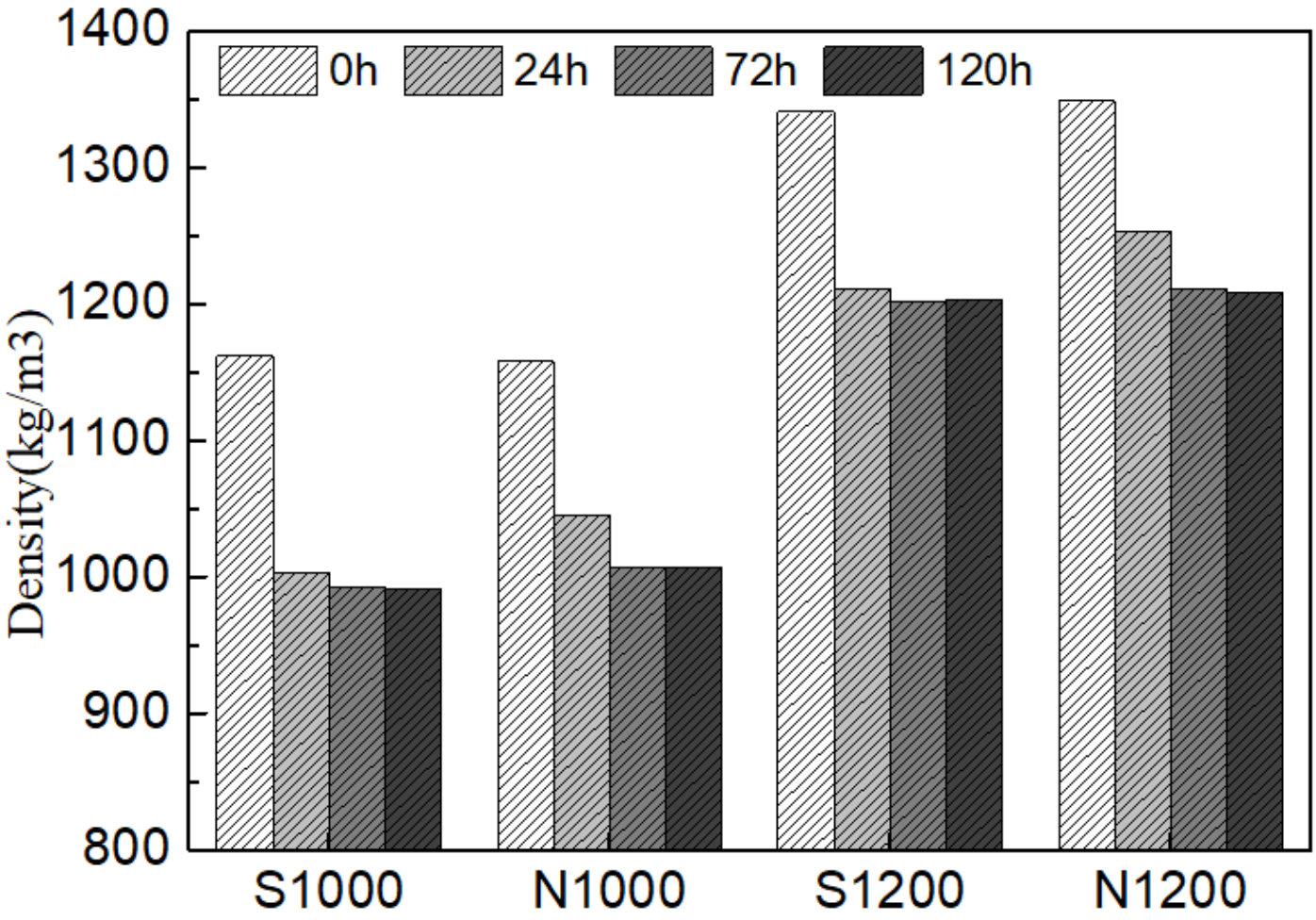

Figure 4

Density of PLAC with CNLA and SLA over 5 d.

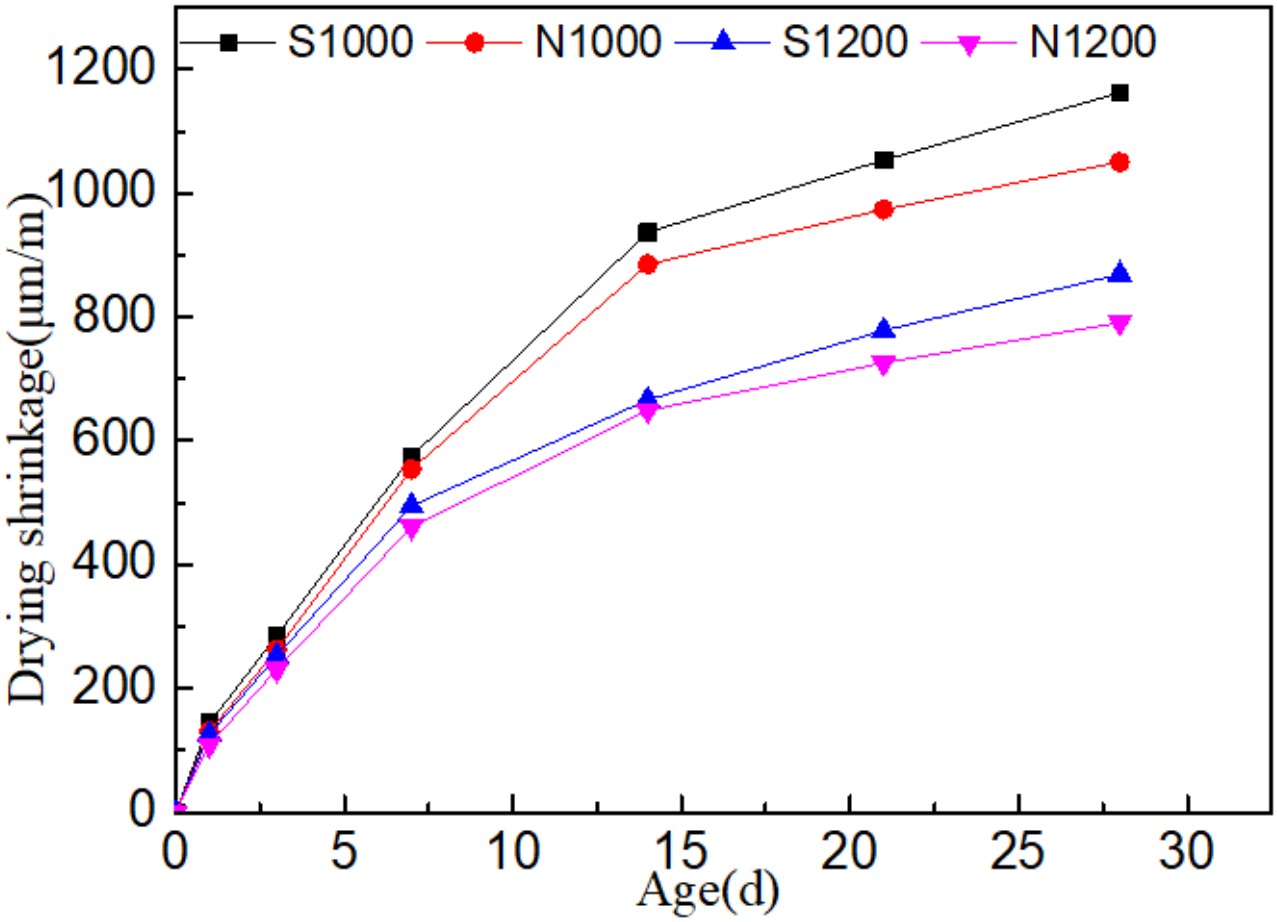

Figure 5

Drying shrinkage of PLAC using CNLA or SLA.

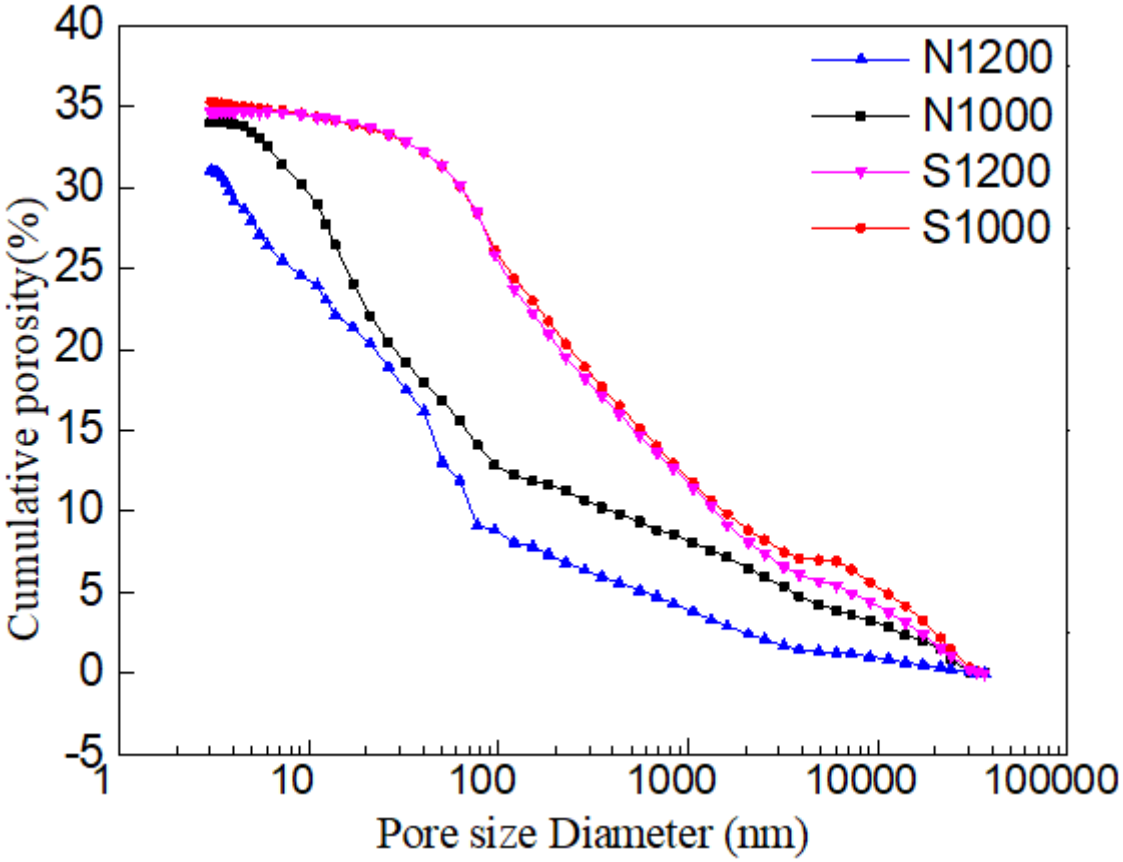

Figure 6

Cumulative porosity of samples: pore size.

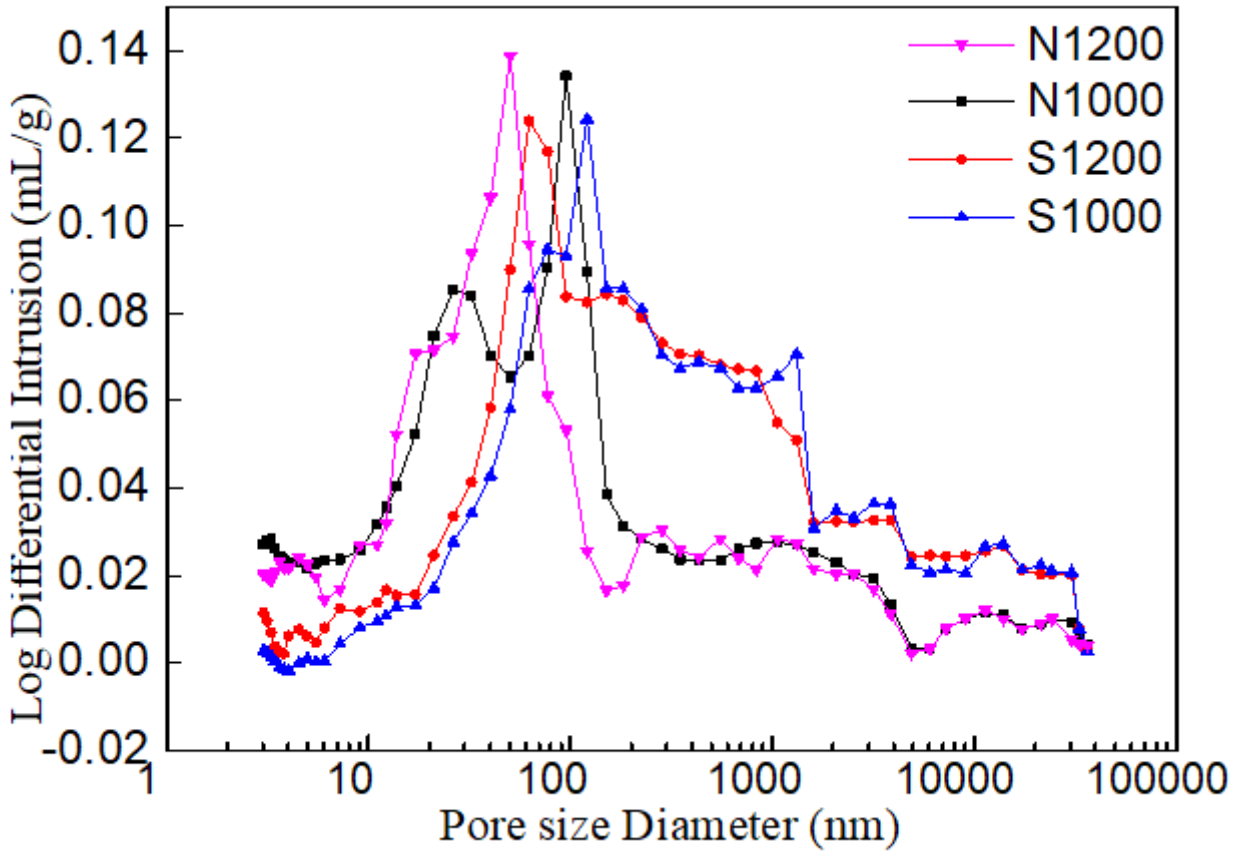

Figure 7

Cumulative porosity of samples: pore size distribution.

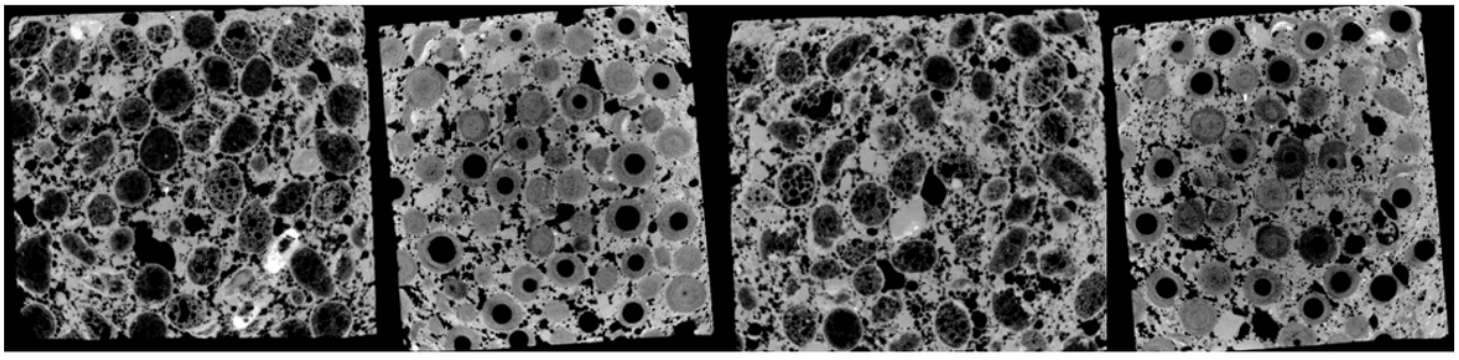

Figure 8

Two-dimensional X-CT slices of concrete specimens.

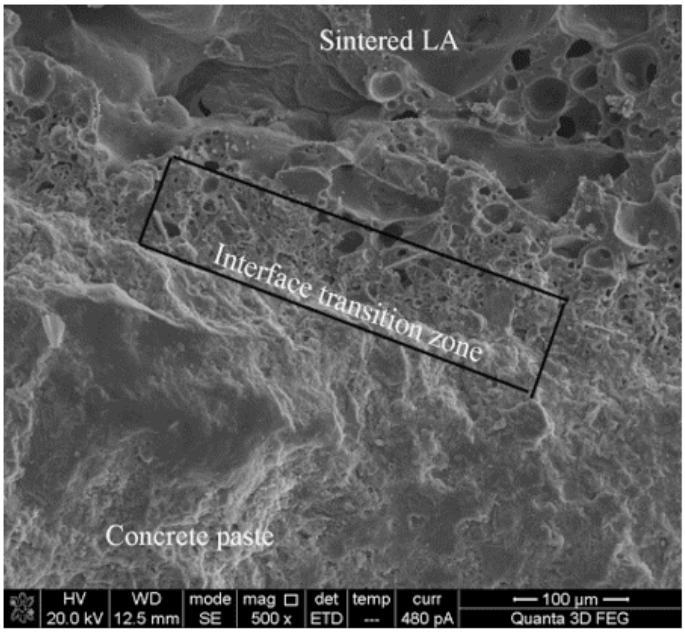

(a) S1200

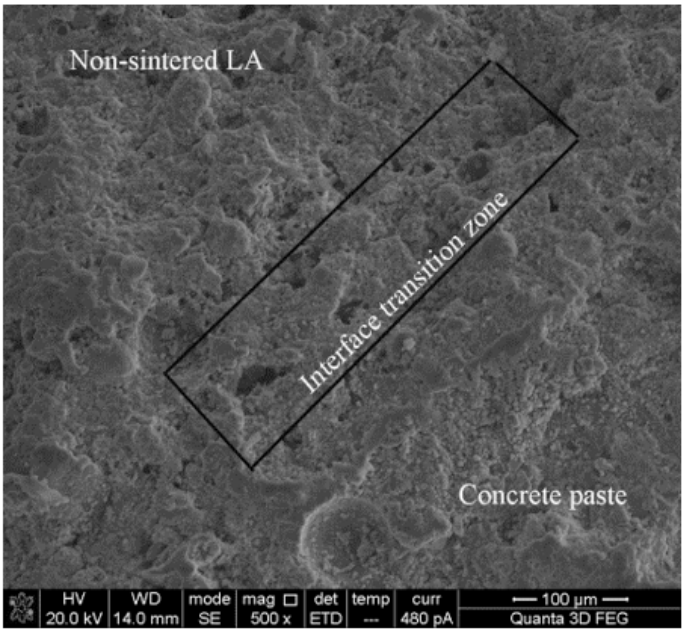

(b) N1200

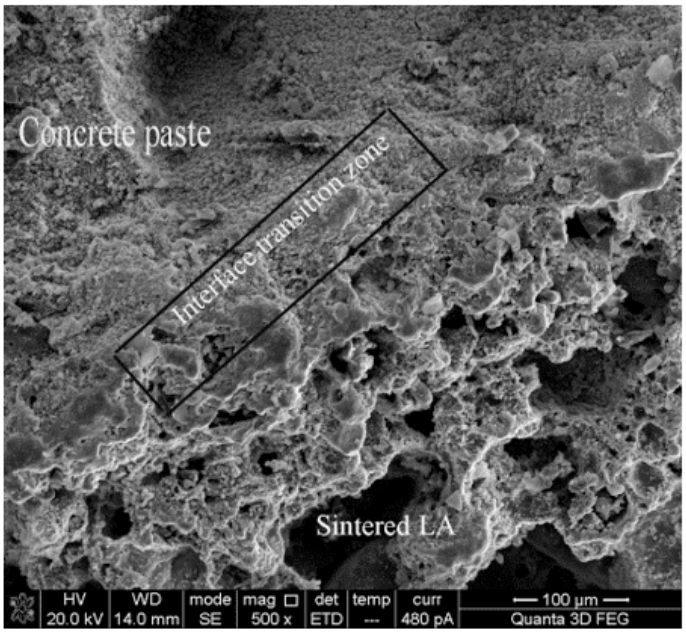

(c) S1000

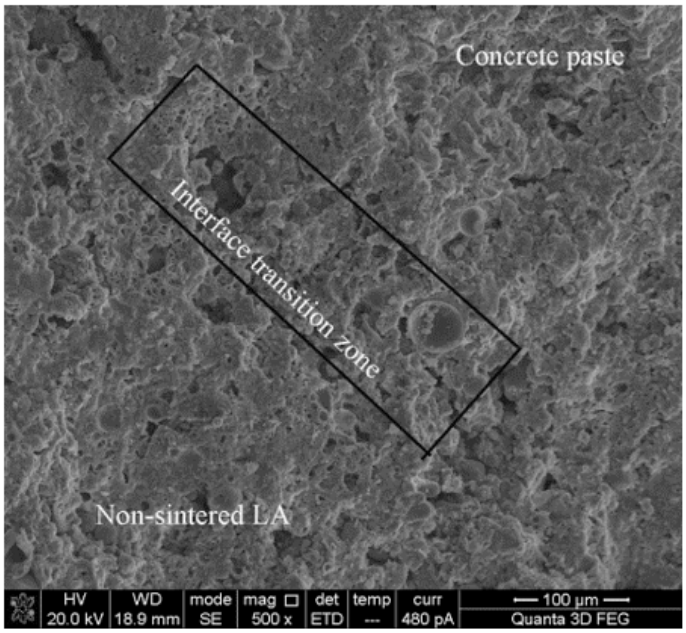

(d) N1000

Figure 9

SEM images of PLAC with CNLA and SLA.